

Research Article

# Thermal Vacuum Process of Dispersing Heterogeneous Materials

Volodymyr Kutovyi\* 

Kharkov Institute of Physics and Technology, Kharkov, Ukraine

## Abstract

The presented work examines physical processes in a thermal vacuum installation, which allow for the effective dispersion of heterogeneous materials within 15 seconds. An analysis of heat and mass transfer processes that affect the dispersion of heterogeneous materials been carried out. Calculations of the speed, frequency and wavelength in spiral heating element of the thermal vacuum installation been made for different angles of motion of material particles. It been established that the speed of motion of a material particle in the cavity of the heating element can be more than a thousand kilometers per second, and the temperature of a local pulsed steam explosion rises to tens of millions of degrees. The results of the study show that during thermal vacuum dispersion of heterogeneous materials, modified nanodispersed materials are formed, neutrinos and transparent glowing bubbles are observed, which appear unexpectedly and as if out of nowhere. The size of the bubbles is (4 ... 5) centimeter. The inner part of the bubble glows with a weak orange-violet color, and closer to the shell, blue color prevails. The reason for the formation of a transparent bubble, apparently, is a local powerful steam explosion with the appearance of a shock wave inside which there is a high temperature and pressure. At the same time, electrification of particles occurs. The voltage of static electrification can reach a value sufficient to tear electrons from atoms. Ionization occurs. At this time, a neutrino and a transparent bubble formed, a gas mixture arises.

## Keywords

Thermal Vacuum Process, Nanodispersed Material, Neutrino, Fermi Bubbles, Intensification

## 1. Introduction

There are many ways to obtain nanodispersed materials, including the method of electron beam evaporation and vacuum deposition [1]. This method is energy-intensive and time-consuming. The development of new functional materials with individual structure and properties is one of the progressive directions of technological progress [2]. During the development of scientific and technological progress, the tasks of developing and mastering innovative types of installations, effective technologies for processing raw materials, obtaining new materials are set. The possibilities of creating

a scalable reproductive process from laboratory research to industrial production are determined. As result of scientific and technical research, a significant amount of experimental material accumulated in the form of new technological processes, characteristics of the resulting product, and device designs [3, 4]. The results of the study show that thermal vacuum dispersion of heterogeneous materials produces neutrinos and transparent glowing bubbles that visually observed in specially made trap. Hereinafter, we will call them Fermi bubbles. The nature of the appearance of neutrinos and Fermi

\*Corresponding author: [kutovoy@kipt.kharkov.ua](mailto:kutovoy@kipt.kharkov.ua) (Volodymyr Kutovyi)

Received: 9 May 2025; Accepted: 26 May 2025; Published: 30 June 2025



Copyright: © The Author(s), 2025. Published by Science Publishing Group. This is an **Open Access** article, distributed under the terms of the Creative Commons Attribution 4.0 License (<http://creativecommons.org/licenses/by/4.0/>), which permits unrestricted use, distribution and reproduction in any medium, provided the original work is properly cited.

bubbles poorly understood. [5, 6]. Dr. Brian Mac Namara, an astronomer from the Ohio University in Athens, believes that the most likely cause of the appearance of Fermi bubbles is powerful explosions of matter based on data obtained from the orbital X-ray observatory "CHANDRA". The mysterious world of neutrinos and Fermi bubbles can tell us a lot about the physical processes that occur in the Universe. Only a detailed study of the process of formation of neutrinos, Fermi bubbles and related phenomena has undoubted scientific value, which will allow us to uncover the mysterious world and identify the physical processes occurring in the Universe. Studying the process of producing neutrinos and Fermi bubbles in a thermal vacuum setup will provide additional information about their properties, interaction with the environment and create new alternative energy sources.

The aim of this work is to develop an efficient thermal vacuum energy-saving, environmentally friendly dispersion of heterogeneous materials and an empirical study of the resulting neutrinos and transparent bubble.

## 2. Thermal Vacuum Process

The experimental methodology of the thermal vacuum process is that for the effective and economical production of nanomaterials it is necessary to ensure a continuous flow of heterogeneous material inside spiral heating element, which has a temperature of 400°C.

The thermal vacuum process based on the principle of combining high-speed evacuation and instantaneous thermal heating of the material inside a hollow heater. [7]. Material enters the cavity of the heating element together with air. A two-phase gas-solid particle system arises. The movement occurs in an upward flow in the heated space with a decrease in pressure. From the results of the experiment established that for continuous operation of the installation and stable movement of particles along the spiral heating it is necessary to observe the condition. The weight of solid particles in one liter of air at the inlet to the cavity of the heating element should be no more than (1.0 – 1.2) g, which should not exceed the standard value of air density. The air density is 1.2255 kg/m<sup>3</sup>, corresponding to the density of dry air at 15 °C and a pressure of 101330 Pa. (Reference data). This due to the fact that the thermal vacuum process forms a significant number of nano-dispersed and finely dispersed particles moving in a unit of volume, increasing their speed of movement and heating temperature. The composition and heat capacity of the environment changes, which leads to a change in the wave motion of the particles. It is necessary that during the process of thermal vacuum dispersion, a uniform density of the substance within the volume maintained, which allows nanodispersed particles to move freely without colliding with each other and allows them to overtake moving particles at a lower speed.

## 3. Analysis of Heat and Mass Exchange Processes in Thermal Vacuum Unit

The dispersed material moving in the cavity of the heating element along the spiral channel subjected to a centrifugal force  $F$

$$F = \frac{m \cdot v^2}{R} \quad (1)$$

where  $m$  is the mass of a particle of dispersed material, kg;  $v$  is the speed of movement of a particle of dispersed material, m/s;  $R$  is the radius of the spiral of the heating element, m.

The centrifugal force presses the particles of the dispersed material against the wall of the heating element. Contact formed between the surface plane of the wet material and the wall of the heater, which allows for maximum use of the heat of the heating element. An instantaneous process of transferring thermal energy from the wall of the heater to the wet material occurs. [8]. Surface element  $dS$  (m<sup>2</sup>) of the wet material receives a powerful flow of thermal energy  $dQ$  (J) with a temperature  $T$  (K) in a short period of time  $\Delta\tau$  (s) with a heat transfer coefficient of  $a$ , (W/m<sup>2</sup> K).

$$dQ = a \cdot T \cdot d\tau \cdot dS \quad (2)$$

Thermal resistance  $R_c$  of the surface layer determines the thickness of thermal energy penetration into the wet material.

$$l = k \cdot R_c \cdot dS \quad (3)$$

where  $l$  is the thickness of thermal energy penetration into a wet body, m;  $k$  is the thermal conductivity coefficient of the material, W/m·K;  $R_c$  is the thermal resistance, K/W.

Substituting the value  $dS$  from expression (2) into expression (3), we obtain the thickness of thermal energy penetration  $dQ$  into a wet body, over a certain of time  $d\tau$ .

$$l = \frac{k \cdot R_c \cdot dQ}{a \cdot T \cdot d\tau} = \frac{k \cdot R_c \cdot P}{a \cdot T} \quad (4)$$

where  $P = dQ/d\tau$  the thermal power received by the surface layer of the material from the wall of the heater during contact, W.

We determine the heating temperature of the surface layer of a material particle.

$$T = \frac{k \cdot R_c \cdot dQ}{a \cdot l \cdot d\tau} = \frac{k \cdot R_c \cdot P}{a \cdot l} \quad (5)$$

It follows from expression (5) that the temperature ( $T$ ) inside the surface layer of the wet material depends on the thermal conductivity coefficient ( $k$ ) and thermal resistance of the material ( $R_c$ ), thermal power ( $P$ ) of the heating element, heat transfer coefficient ( $a$ ) of the material, thickness ( $l$ ) of the surface layer. The temperature ( $T$ ) of the surface layer of the wet material at moment of contact with the wall of the

heater becomes significantly higher than the temperature ( $T_1$ ) of evaporation of moisture, which is in the surface layer ( $T \gg T_1$ ). Instantaneous overheating of the liquid occurs. The process of intensive vaporization begins in the surface layer at the pressure ( $P_1$ ) of the environment. The pressure ( $P_1$ ) in the cavity of the heating element created by vacuum pump. As result of intensive vaporization, the pressure of saturated vapor ( $P_2$ ) inside the surface layer becomes significantly higher than on the surface ( $P_2 \gg P_1$ ). Thus, in the surface layer, at the moment of contact of the wet material with the hot wall of the heating element, a concentration of thermal energy occurs, which leads to the formation of a local pulse steam explosion in a limited space [9]. A shock wave formed, inside which the temperature and pressure increase. [10]. Process of crushing the surface layer of the material occurs. At this moment, each particle detached from the main mass acquires kinetic energy. In the case under consideration, the kinetic energy of the particle depends on the thermal energy ( $Q$ ) it receives from the heating element in a short period time.

$$Q = dm \cdot c \cdot (T_3 - T_4) = dm \cdot c \cdot \Delta T = \frac{dm \cdot v^2}{2}, \quad (6)$$

where  $c$  is the heat capacity material,  $J/kg \cdot K$ ;  $T_3$  the instantaneous heating temperature of the surface layer with a mass of  $dm$  when the body touches the heating element,  $K$ ;  $T_4$  is the initial temperature of the surface layer of the body,  $K$ ;  $\Delta T$  is the difference between the initial and final heating temperatures of the surface layer. That is, the kinetic energy of particle is equivalent to the thermal energy ( $Q$ ) received by the surface layer or a separate particle with a mass of  $dm$  the moment of contact with the wall of the heating element.

$$dm \cdot c \cdot \Delta T = \frac{dm \cdot v^2}{2} \quad (7)$$

After transforming expression (7), we obtain

$$\Delta T = \frac{v^2}{2c} \quad (8)$$

From expression (8) it follows that the temperature obtained by the surface layer or a separate particle of the material when touching the wall of the heating element is directly proportional to the square of the body velocity and inversely proportional to its heat capacity. The higher the temperature of the surface layer of the material body in a short period time, the more powerful the local pulsed steam explosion and the higher the speed of movement of small particles. When a particle of the material touches the wall of the heating element, a shock wave front is formed, which is characterized by extremely high values of excess pressure and high temperature. [11]. Duration of the shock wave is  $(2...10) \cdot 10^{-3}$  s. [12]. In pulsed shock wave, irreversible processes occur so quickly that polymorphic transformations vary within extremely wide limits. As a result, the particles that have bro-

ken away from the main mass will be in close proximity to the shock wave, and will receive a powerful force impact, which leads to an increase in their temperature, further fragmentation with the formation of numerous fragments of various shapes and masses with an increase in the total surface area. [8]. New crystalline modifications arise, which affected by the force of traction ( $F_T$ ).

$$F_T = m \cdot a_1 \quad (9)$$

where  $a_1$  acceleration of the body particles,  $m/s^2$ .

When a material particle moves towards the wall of the heating element in the opposite direction of the centrifugal force, then in this case the thrust force must be greater than the centrifugal force ( $F_T > F$ ). If the particle's motion is directed towards the centrifugal force, then the force

$\Sigma (F_T + F)$  acts on it. Let's assume that the thrust force at some point in time is equal to the centrifugal force ( $F_T = F$ ), then,

$$m \cdot a_1 = \frac{m \cdot v^2}{R}; \quad \frac{m \cdot v}{\tau^2} = \frac{m \cdot v^2}{R}, \quad (10)$$

where  $\tau$  is the time of influence of the temperature of the heating element on the material particle during its contact with the heater wall, s.

From expression (10) we obtain,

$$\tau = \sqrt{\frac{R}{v}} \quad (11)$$

Therefore, the time of contact of a material particle with the wall of the heating element is equal to the square root of the radius of the heating element divided by the speed of movement.

All this mass moves at different speeds in the heater cavity. At this time, the electrification of particles occurs, large and small particles acquire charges of opposite signs. [13]. Voltage of static electrification can reach a value sufficient to separate electrons from atoms, resulting in ionization. This contributes to the formation of a new crystalline modification of matter, neutrino flux and Fermi bubbles. At the same time, the rest of the material particles, which are located outside the shock wave, are in a metastable state.

## 4. Determination of the Velocity of a Material in the Heating Element Cavity

If the body moves linearly inside the heating element, then its speed is 6.7 m/s. However, during movement in the cavity of spiral heating element of the thermal vacuum installation, the material particle moves in a zigzag manner from one wall to the other. In connection with which the speed of its movement in the thermal vacuum installation will depend on

the angle of movement to the opposite wall of the heater and on the length of the path traveled.

Let us calculate the speed of movement of a body particle at different angles of movement to the opposite wall of the spiral heater. From the place (C), the supposed contact of the body with the heater wall, we will establish a perpendicular to the opposite wall of the heater (Figure 1).

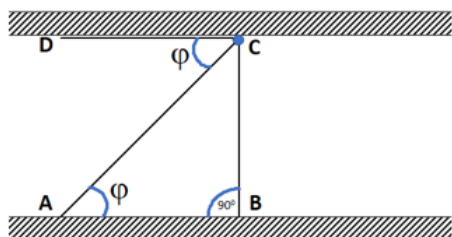


Figure 1. One of the possible movements of a particle of dispersed material from one wall to the opposite wall in the cavity of the heating element

From point (C) draw a line at an angle ( $\varphi$ ) to the opposite wall of the heater. We get a right triangle ABC. The side BC of the right-angled triangle ABC is equal to the inner diameter of the heating element ( $d$ ), and the side AB is equal to the part of the wall of the heating element. It assumed that at this moment the movement of the body in the cavity of the heating element from one wall to the other occurs along the hypotenuse AC at an angle of incidence ( $\varphi$ ) to the opposite wall of the heater. In this case, the hypotenuse AC of the right-angled triangle has the size

$$AC = \frac{BC}{\sin\varphi} = \frac{d}{\sin\varphi} \tag{12}$$

Let's calculate side AB.

$$AB = \sqrt{AC^2 - BC^2} = \sqrt{\left(\frac{d}{\sin\varphi}\right)^2 - d^2} = \sqrt{\frac{d^2 \cdot \cos^2\varphi}{\sin^2\varphi}} = d \cdot \text{Ctg}\varphi \tag{13}$$

Will determine how many times segment AC is larger segment AB. The path traveled by a material particle will be that many times greater than in rectilinear motion, and the speed of its movement will be that many times greater.

$$\frac{AC}{AB} = \frac{d}{\sin\varphi \cdot d \cdot \text{Ctg}\varphi} = \frac{1}{\sin\varphi \cdot \text{Ctg}\varphi} = \frac{\sin\varphi}{\sin\varphi \cdot \cos\varphi} = \frac{1}{\cos\varphi} \tag{14}$$

In our case

$$\lambda = 2AB = 2 \cdot d \cdot \text{Ctg}\varphi \tag{15}$$

$\lambda$  the wavelength, m.

Then the velocity of the particle of the body will be accordingly

$$v = 6,7 \frac{1}{\cos\varphi} = \frac{6,7}{\cos\varphi} \tag{16}$$

Let us determine the frequency of oscillation of a body particle depending on the angle of motion

$$f = \frac{v}{\lambda} = \frac{6,7}{2d \cdot \text{Ctg}\varphi \cdot \cos\varphi} \tag{17}$$

where  $f$  is the frequency, Hz.

The results of the calculations, within the permissible error, given in the table, in which:

$\varphi$  motion angle of the material particle;  $v$  velocity of motion particles, m/s;

$\lambda$  wavelength, m;  $f$  frequency of oscillations, Hz.

Table 1. Calculation of the speed, frequency, wavelength in the heating element of a thermal vacuum installation for different angles of motion of material particles.

$\varphi$	89°59'59"	89°59'58"	89°59'57"	89°59'56"	89°59'55"	89°59'54"	89°59'53"	89°59'52"	89°59'51"
$v, \text{ m/c}$	$1,4 \cdot 10^6$	$6,9 \cdot 10^5$	$4,5 \cdot 10^5$	$3,5 \cdot 10^5$	$2,8 \cdot 10^5$	$2,3 \cdot 10^5$	$2,0 \cdot 10^5$	$1,7 \cdot 10^5$	$1,5 \cdot 10^5$

$\varphi$	89°59'59"	89°59'58"	89°59'57"	89°59'56"	89°59'55"	89°59'54"	89°59'53"	89°59'52"	89°59'51"
$\lambda, \text{ м}$	$0.24 \cdot 10^{-6}$	$0.46 \cdot 10^{-6}$	$0.73 \cdot 10^{-6}$	$0.95 \cdot 10^{-6}$	$0.12 \cdot 10^{-5}$	$0.14 \cdot 10^{-5}$	$0.17 \cdot 10^{-5}$	$0.19 \cdot 10^{-5}$	$0.21 \cdot 10^{-5}$
$f, \text{ Гц}$	$5.8 \cdot 10^{12}$	$1.5 \cdot 10^{12}$	$6,2 \cdot 10^{11}$	$3,7 \cdot 10^{11}$	$2,3 \cdot 10^{11}$	$1,6 \cdot 10^{11}$	$1,2 \cdot 10^{11}$	$9,0 \cdot 10^{10}$	$7,2 \cdot 10^{10}$
$\varphi$	89°59'50"	89°59'49"	89°59'30"	89°59'	89°58'59"	89°57'	89°56'	89°55'	89°54'
$v, \text{ м/с}$	$1,37 \cdot 10^5$	$1,25 \cdot 10^5$	$4,6 \cdot 10^4$	$2,3 \cdot 10^4$	$2,26 \cdot 10^4$	$7,5 \cdot 10^3$	$5,7 \cdot 10^3$	$4,6 \cdot 10^3$	$3,8 \cdot 10^3$
$\lambda, \text{ м}$	$0.23 \cdot 10^{-5}$	$0.26 \cdot 10^{-5}$	$0.8 \cdot 10^{-5}$	$1.4 \cdot 10^{-5}$	$1.42 \cdot 10^{-5}$	$0.42 \cdot 10^{-4}$	$0.56 \cdot 10^{-4}$	$0.7 \cdot 10^{-4}$	$0.8 \cdot 10^{-4}$
$f, \text{ Гц}$	$5,9 \cdot 10^{10}$	$4,8 \cdot 10^{10}$	$5.7 \cdot 10^9$	$1.6 \cdot 10^9$	$1.59 \cdot 10^9$	$1.8 \cdot 10^8$	$1.0 \cdot 10^8$	$6.6 \cdot 10^7$	$4.8 \cdot 10^7$
$\varphi$	89°53'	89°52'	89°50'	89°47'	89°45'	89°30'	89°25'	89°21'	88°59'59"
$v, \text{ м/с}$	$3,2 \cdot 10^3$	$2,8 \cdot 10^3$	$2,3 \cdot 10^3$	$1,8 \cdot 10^3$	$1,5 \cdot 10^3$	$7,7 \cdot 10^2$	$6,6 \cdot 10^2$	$5,9 \cdot 10^2$	$3,8 \cdot 10^2$
$\lambda, \text{ м}$	$0.98 \cdot 10^{-4}$	$0.11 \cdot 10^{-3}$	$0.14 \cdot 10^{-3}$	$0.18 \cdot 10^{-3}$	$0.2 \cdot 10^{-3}$	$0.42 \cdot 10^{-3}$	$0.48 \cdot 10^{-3}$	$0.54 \cdot 10^{-3}$	$0.84 \cdot 10^{-3}$
$f, \text{ Гц}$	$3,3 \cdot 10^7$	$2,5 \cdot 10^7$	$1,6 \cdot 10^7$	$9.8 \cdot 10^6$	$7.5 \cdot 10^6$	$1.8 \cdot 10^6$	$1.3 \cdot 10^6$	$1.1 \cdot 10^6$	$4,5 \cdot 10^5$
$\varphi$	88 °	87 °	86 °	85 °	84 °	83 °	82 °	81 °	80 °
$v, \text{ м/с}$	$1,9 \cdot 10^2$	$1,3 \cdot 10^2$	96	77	65	54	48	43	39
$\lambda, \text{ м}$	$1.7 \cdot 10^{-3}$	$2.6 \cdot 10^{-3}$	$3.4 \cdot 10^{-3}$	$4.2 \cdot 10^{-3}$	$5.0 \cdot 10^{-3}$	$6.0 \cdot 10^{-3}$	$6.8 \cdot 10^{-3}$	$7.6 \cdot 10^{-3}$	$8.5 \cdot 10^{-3}$
$f, \text{ Гц}$	$1,1 \cdot 10^5$	$5,1 \cdot 10^4$	$2,9 \cdot 10^4$	$1,8 \cdot 10^4$	$1,3 \cdot 10^4$	$9 \cdot 10^3$	$7 \cdot 10^3$	$5.6 \cdot 10^3$	$4.5 \cdot 10^3$
$\varphi$	75 °	70 °	65 °	60 °	55 °	50 °	45 °	40 °	30 °
$v, \text{ м/с}$	23,2	19,6	15,9	13,4	11,7	10,4	9,5	8,8	7,7
$\lambda, \text{ м}$	$1,3 \cdot 10^{-2}$	$1,8 \cdot 10^{-2}$	$2,2 \cdot 10^{-2}$	$2,8 \cdot 10^{-2}$	$3,4 \cdot 10^{-2}$	$4,0 \cdot 10^{-2}$	$4,8 \cdot 10^{-2}$	$5,7 \cdot 10^{-2}$	$8,3 \cdot 10^{-2}$
$f, \text{ Гц}$	$1,8 \cdot 10^3$	$1,1 \cdot 10^3$	$7,1 \cdot 10^2$	$4,8 \cdot 10^2$	$3,5 \cdot 10^2$	$2,6 \cdot 10^2$	$2,0 \cdot 10^2$	$1,5 \cdot 10^2$	93
$\varphi$	20 °	15 °	10 °	5 °	4 °	3 °	2 °	1 °	0 °
$v, \text{ м/с}$	7,1	6,9	6,8	6,73	6,72	6,71	6,7	6,7	6,7
$\lambda, \text{ м}$	0,13	0,18	0,27	0,55	0,69	0,92	1,4	2,8	-
$f, \text{ Гц}$	53,8	38,7	25,0	12,3	9,8	7,3	4,9	2,4	-

From the calculation results it follows that when moving at an angle  $\varphi = 89^\circ 59' 59''$  to the opposite wall of the heating element, the material particle moves with a speed of 1400 km/s and a frequency of  $5.8 \cdot 10^{12}$  Hz. The wavelength is  $0.24 \cdot 10^{-6}$  m. According to expression (11), the time of influence of the temperature of the heating element on the material particle during its contact with the wall at a speed of its movement of 1400 km/s is  $6 \cdot 10^{-4}$  s, and the local temperature of heating of microparticles in the pulse, according to expression (8), can reach 34 million degrees.

If the blast wave is directed towards the opposite wall of the heating element at an angle of  $\varphi = 89^\circ 59' 58''$ , then together with the blast wave moves a finely dispersed material, the size of which does not exceed the wavelength of  $0.48 \cdot 10^{-6}$  m with an oscillation frequency of 1.4 THz and a speed of 670 km/s. The time of influence of the temperature of the heating element on the material particle during its contact with the wall is  $8.6 \cdot 10^{-4}$  s. From the calculation results it follows that a change in the angle of the direction of movement of a nanodispersed particle by one second in the range

( $89^\circ 59' 58'' \dots 89^\circ 59' 59''$ ) increases its speed by approximately 2.0 times, and the oscillation frequency by 3.9 times.

Changing the angle of the direction of movement of a material particle to the opposite wall of the heating element in the range ( $89^\circ 58' 59'' \dots 89^\circ 59' 59''$ ) in one minute increases the speed of movement by 62 times, and the oscillation frequency by  $3.6 \cdot 10^3$  Hz.

Changing the direction of movement of a material particle to the opposite wall of the heating element by one degree in the range ( $88^\circ 59' 59'' \dots 89^\circ 59' 59''$ ) increases its speed of movement by  $3.6 \cdot 10^3$  times, and the oscillation frequency by  $1.3 \cdot 10^7$  Hz. Therefore, a material particle that has changed its speed of movement, mass, size can move from one frequency range to another frequency range and change the angle of movement, which ensures energy-efficient, high-performance continuous dispersion of the material in a vacuum environment.

According to expression (8), the two-phase flow is heated to 100°C at a speed of 590 m/s. and the angle of motion between the heater walls  $\varphi = 89^\circ 21'$ . At this time, the specific

heat capacity of the two-phase flow is the sum of the heat capacities of carbon and air. The effect of the temperature of the heating element on a material particle during its contact with the wall is  $3.0 \cdot 10^{-2}$ s.

From the results given in the table, it follows that in the range of angles  $\varphi = (80^\circ \dots 50^\circ)$  particles with a size of 8.5 mm to 40 mm can move, and the speed of movement of these particles exceeds the acceleration of a freely falling body.

In the range of angles from  $21^\circ$  and almost to  $50^\circ$ , the movement of material particles is chaotic. The speed of movement is lower than the acceleration of a freely falling body. The particles pass from laminar motion to turbulent motion. At this time, the temperature of the material particle increases due to partial contact with the wall of the heating element and the flow of thermal radiation coming from the wall of the heating element.

In the range of angles  $\varphi = (20^\circ \dots 0^\circ)$  the movement of heterogeneous material in the heating element occurs almost rectilinearly, i.e. the flow is laminar. Fine particles are not in the front of the shock wave at this time they only affected by the flow of thermal radiation, which comes from the wall of the heating element.

If a nanodispersed particle moves to the opposite wall of the heater at an angle  $\varphi = 90^\circ$ , then the route it has traveled in time will be the same, that is, the part is in a potential well. But this not happen because the phase shift for nanodispersed particles creates a flow of the environment, which is formed by a vacuum pump, which is an analogue of a black hole, where all material particles strive. Therefore, each newly created material particle in the heating element of a thermal vacuum installation moves along its trajectory at a strictly defined angle has its own frequency of movement, speed, and mass.

## 5. Carbon Dispersion Process

We will conduct experimental studies of the thermal vacuum process of dispersing heterogeneous materials in a thermal vacuum installation. Let us consider the process of processing carbon grade C1. The initial size of carbon particles is 6 mm, humidity 5.8%. To obtain an image of the crystal structure and surface of the object with high spatial resolution, as well as for a detailed examination of the structure of nanographite obtained in a thermal vacuum installation, scanning and transmission electron microscopes used.

In a thermal vacuum installation, nanodispersed single-layer graphite with a size of (10...40) nm was obtained (Figure 2).

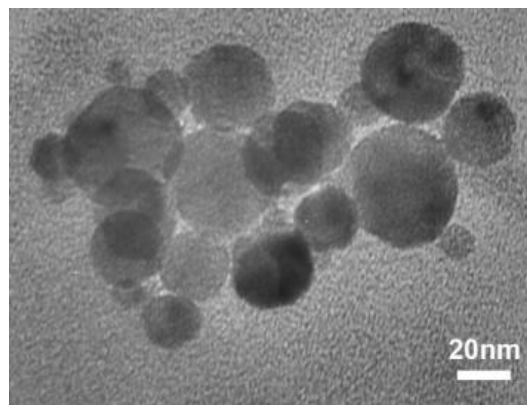


Figure 2. Nanodispersed graphite, single-layer.

During the thermal vacuum process, a locally pulsed carbon microexplosion occurs, leading to the modification of new carbon materials. The matter transitions from one form to another. Figure 3 Shows reciprocal lattice of a nanodispersed graphite particle of the C1 grade, which has a normal hexagonal shape with its reflection in the basic crystallographic plane.

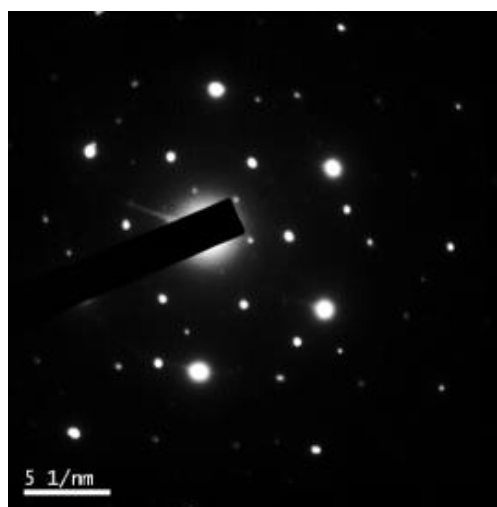


Figure 3. Hexagonal, graphite lattice.

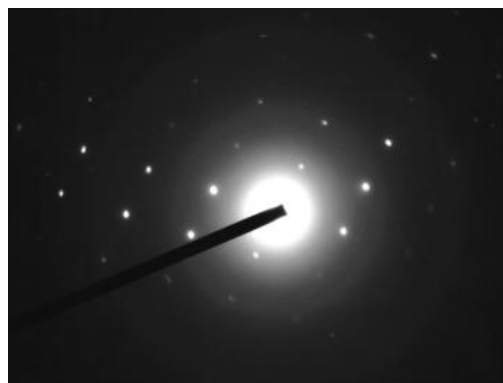


Figure 4. Monoclinic modification of the graphite lattice.

Based on graphite C1, processed in a thermal vacuum installation, a monoclinic modification of the reciprocal lattice with an angle  $\beta = 99^{\circ}5'$  was discovered. Figure 4. All this confirmed by the intensity diagram of X-ray reflections of graphite C1 in the initial and heat-treated state. Figure 5.

Thus, the thermal vacuum process makes it possible to obtain nanodispersed modifications of new carbon materials with minimal energy costs in 15 seconds. In the process of dispersing carbon in a specially made trap, neutrino fluxes

and Fermi bubbles visually observed. Fermi bubbles appear unexpectedly and as if from nowhere. Their size is (4...5) cm. The inner part of the bubble glows with a weak orange-violet color, and closer to the shell, the blue color prevails. All this observed visually. In the future, all this be studied more carefully and filmed a high-speed camera. In the process of dispersing, it is also necessary to study gas evolution and determine their composition and quantity. For now, these are preliminary observations.

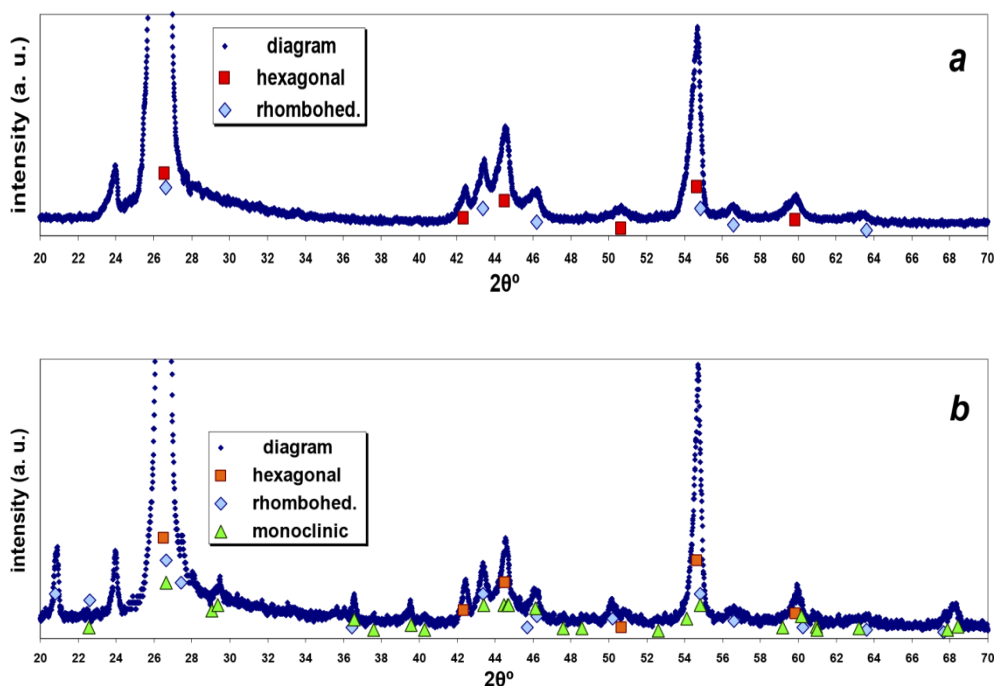


Figure 5. Fragments of the X-ray diagram with designations of calculated prints from the components of graphite C1. Initial (a). Processed in a thermal vacuum installation (b).

## 6. Thermal Vacuum Process for Obtaining Zirconium Dioxide

As is known, one of the most common methods for obtaining nanodispersed zirconium dioxide powders hydrothermal. [14]. However, the described method allows obtaining nanodispersed zirconium dioxide in aqueous, acidic and alcoholic solutions for a long time.

The thermal vacuum process forms finely dispersed zirconium dioxide directly from zirconium hydroxide, without aqueous, acidic and alcoholic additives. The residence time of the starting material in the thermal vacuum unit is 15 seconds. [15].

To study the thermal vacuum process, zirconium hydroxide with a particle size of the order of (10...2) mm and a humidity of 12.5% was taken. As a result of the thermal vacuum process, pure zirconium dioxide is formed from zirconium hydroxide in an amorphous state of randomly oriented crystallites with a humidity of 1.8%, with a porous structure

with a size of (20...200) nm, a developed specific surface area and a large volume of sorption space. Figure 6.

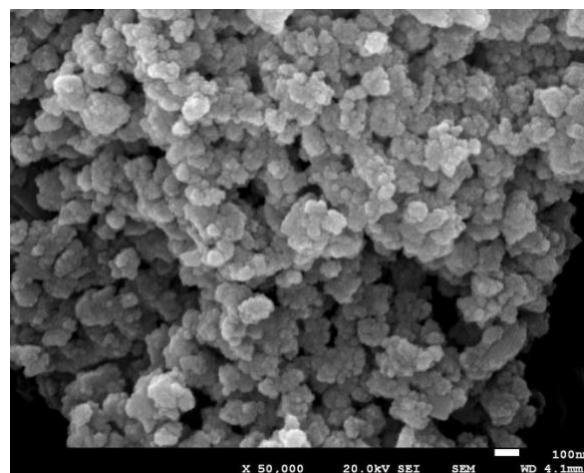
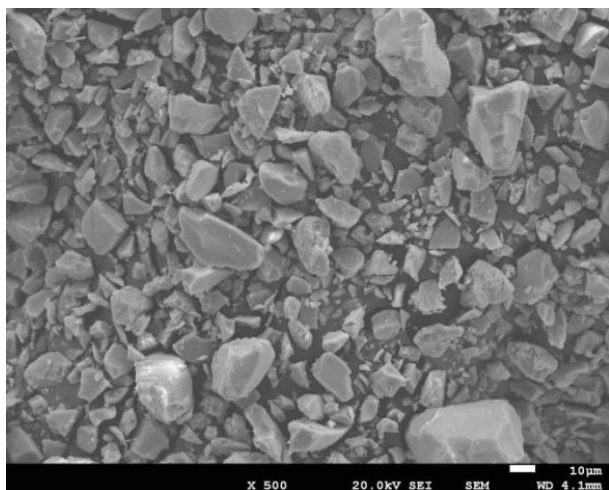


Figure 6. Amorphous zirconium dioxide.



**Figure 7.** Crystalline zirconium dioxide.

Simultaneously with amorphous zirconium dioxide, finely dispersed crystalline zirconium dioxide also obtained in the thermal vacuum installation. **Figure 7.** Thus, the thermal vacuum process forms crystallographic modifications of the material. Amorphous zirconium dioxide retained by a fine filter. Crystalline fractions were retained a coarse filter. As a result, amorphous zirconium dioxide obtained with a yield of 30% of the total mass, with a bulk density of  $1.64 \text{ g/cm}^3$ , while the bulk density of zirconium hydroxide was  $1.05 \text{ g/cm}^3$ . Thus, by analyzing the obtained results of the thermal vacuum process of nanodispersed materials, it is possible to determine the mechanisms of influence on the object under study and create a highly efficient technological method for the formation of nanodispersed materials.

## 7. Conclusions

- 1) According to the results of the conducted research, it was established. The speed of movement of material particles in the cavity of spiral heating element of the thermal vacuum installation depends on the power of the local pulse steam explosion with the occurrence of a shock wave and due to the energy of thermal radiation of the heater walls. The greater the speed of movement of a material particle, the smaller its mass, the greater the angle of incidence of the particle on the opposite wall of the heater. The speed of movement can reach more than a thousand kilometers per second. At same time, the pulse temperature of the medium increases, the kinetic energy of the material particles increases, the flows of electrons, protons and other charged particles significantly accelerated. Nanodispersed material formed, neutrino flow Fermi bubble arise.
- 2) Heterogeneous materials in a thermal vacuum installation sequentially subjected to force, thermal, deformation, and ionization effects in a short period of time,

which significantly accelerates the process of obtaining nanodispersed materials with new physicochemical mechanical properties, and forms a neutrino flux and Fermi bubbles. Each physical process in the heating element has its own space-time continuum and it is necessary to take into account only those parameters that correspond to a certain interaction.

- 3) The thermal vacuum method creates the prerequisites for obtaining charged particles and a neutrino flux. Neutrinos move from the heating element of the thermal vacuum installation to a specially made trap, where they currently recorded visually. Therefore, in the future it is possible to study the appearance of neutrinos and Fermi bubbles using a small-sized energy-saving thermal vacuum installation without large financial costs and significant difficulties.
- 4) Existing methods for constructing a new crystal lattice require complex rearrangements of atoms, energy costs, and a long time to overcome huge activation barriers from several eV to tens of eV. In a thermal vacuum installation, using thermal diffusion and a pulsed shock wave, crystalline modifications of materials with new properties arise in a few milliseconds with minimal energy costs.
- 5) The thermal vacuum process is a progressive means of obtaining nanodispersed materials: it increases the efficiency of thermotechnical equipment, reduces energy consumption, reduces the time of obtaining nanodispersed materials, and reduces the cost of the technological process. The results of the study can used for the effective continuous production of new nanomaterials, detailed study of the process of obtaining neutrino flux and Fermi bubbles.

## Abbreviations

Intensity (a. u.)    Intensity (Conventional Units)

## Author Contributions

Volodymyr Kutovyi is the sole author. The author read and approved the final manuscript.

## Conflicts of Interest

The author declares no conflicts of interest.

## References

- [1] B. A. Movchan Electron Beam Technology of Evaporation and Vapor Deposition of Inorganic Materials with Amorphous, Nano- and Microstructure. *Nanosystems, Nanomaterials, Nanotechnologies.* - 2004. - V. 2. No. 4. P. 1103 – 1126.

- [2] S. D. Jadhav, I. A. Shaikh. Nanoparticles Synthesis Overview, Review Article. International Journal of Trend in Scientific Research and Development (IJTSRD), Issue: 3. 2019. P. 426 - 428.
- [3] V. P. Vinnikov, M. B. Generalov. Methods for Obtaining Nanodispersed Powders. Profession. 2016. 240 p.
- [4] T. E. Konstantinova, I. A. Danilenko, V. V. Tokiy, V. A. Glazunova. Obtaining Nanosized Powders of Zirconium Dioxide. From Novation to Innovation. Science and Innovation. 2005. V 1. No. 3. P. 76–87.
- [5] W. Hillebrandt, J. C. Niemeyer. Type Ia Supernova Explosion Models // Annual Review of Astronomy and Astrophysics. 2000. Vol. 38. P. 191—230.
- [6] Su. M. Slatyer, T. R. Finkbeiner, D. P. Giant. Gamma-ray Bubbles from Fermi-LAT: Active Galactic Nucleus Activity or Bipolar Galactic Wind? *Astrophys. J.* 2010. 724. P. 1044–1082.
- [7] Apparatus for drying of wet dispersed raw materials. Kutovyi Volodymyr. Patent number W0/2007/013866 (A1). Claimed: 15. 01. 2005. Published: 01.02.2007. Application number WO2005UA00051 20051115. Priority document number: UA200550007488 20050727.
- [8] V. Kutovyi. Physical Processes in the Thermal Vacuum System. American Journal of Physics and Applications. Vol. 10. No. 1. 2022. P. 1-7.
- [9] N. V. Bulanov. Explosive boiling of dispersed liquids. Ekaterinburg. 2011. 232 p.
- [10] L. D. Landau, E. D. Lifshits. Hydrodynamics. M. Fizmatlit, 2001. 736 p.
- [11] N. N. Sysoev, F. V. Shugaev. Shock waves in gases and condensed media. M. University. 1987. 133 p.
- [12] Ya. B. Zeldovich, Yu. P. Raizner. Physics of shock waves and high-temperature hydrodynamic phenomena. M. Nauka. 1966. 686p.
- [13] G. A. Mesyats, Yu. I. Bychkov, V. V. Kremnev. Pulsed nanosecond electric discharge in gas. // *Uspekhi fizicheskikh nauk.* 1972. Vol. 107. Iss. 6. P. 201-228.
- [14] A. V. Zhukov, S. V. Chizhevskaya, P. P. Piae, V. A. Panov. Hetero-phase Synthesis of Zirconium Hydroxide from Zirconium Oxochloride // *Inorganic materials.* Vol. 55. No. 10. 2019. P. 1051-1058.
- [15] V. O. Kutovyi, D. G. Malykhin, V. D. Virych, R. L. Vasilenko. Thermal-Vacuum Method for Obtaining Nanodispersed Zirconium Dioxide. *East European Journal of Physics.* No. 4. 2021. - P. 86-90.